Supplementary Information (SI) for ChemComm.
This journal is © The Royal Society of Chemistry 2024

Supporting Information

Multi-interpenetration driven ultra-robust ionic HOF with high proton conductivity for DMFC

Xiang-Tian Bai, Li-Hui Cao*, Yan Yang, Xu-Yong Chen

Shaanxi Key Laboratory of Chemical Additives for Industry, College of Chemistry and Chemical Engineering, Shaanxi University of Science and Technology, Xi'an, 710021, China

E-mail: caolihui@sust.edu.cn

Section S1. Materials and methods

Nafion solution (20 wt%) was obtained from a commercial supplier. H_4TSM[1], and DBpy·2I[2] were synthesized according to public reports. Unless otherwise stated, all starting solvents and materials can be used without further purification. The measurement of powder X-ray diffraction (PXRD) is carried out in Bruker MXIμS micro-source and ApexII CCD detector, the range is 2θ = 5−55º. Thermogravimetric analysis (TGA) is performed on the TGA-55 instrument at room temperature to 800 °C at a heating rate of 10 °C/min in the N_2 atmosphere.

Synthesis of iHOF-12. Water (1 mL) was added to H_4TSM (6.4 mg, 0.01 mmol) and DBpy·2I (8.84 mg, 0.02 mmol) was dissolved in DMF (1 mL). Then the two clear solutions were mixed and left at 40 °C in the drying oven, the yellow bulk crystals gradually grew out. The yield was 68%, based on H_4TSM. IR: 3478 (s), 3261 (m), 1635 (s), 1571 (s), 1492(s), 1220 (s), 613 (m).

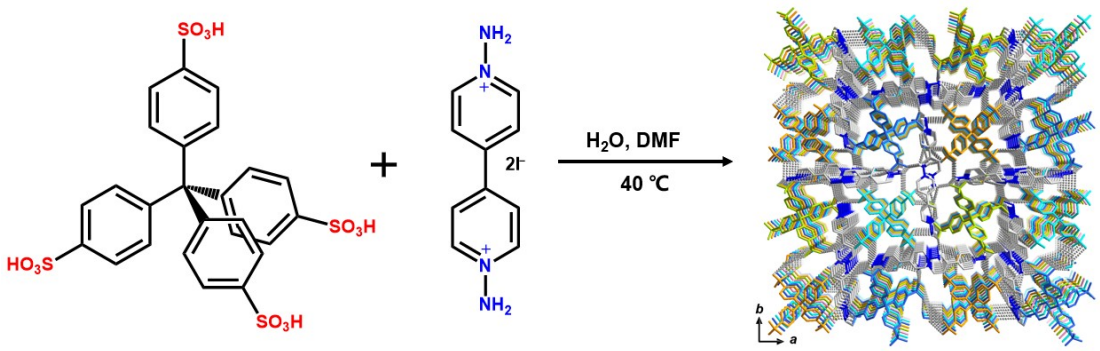

Scheme S1. Schematic representation for preparation of **iHOF-12**.

Preparation of composite membranes. The iHOF (7.5 mg) was first ground to a powder and added to isopropanol (5 mL) with constant stirring. A 20 wt% solution of Nafion (1.5 g) was then added to the suspension and stirred at room temperature for 6 hours to allow sufficient dispersion to obtain the mixture. The resulting mixture was

then poured onto a slide and dried at room temperature until the solvent was removed. Afterward, the composite membranes were soaked with 3 wt% H_2O_2 and 1 M H_2SO_4 solutions for 1 hour at 80 °C, respectively. Finally, the membranes were washed with deionized water until neutral and dried to obtain **2.5%-iHOF-12/Nafion** membranes for testing. The 5.0% and 7.5% composite membranes were prepared in a similar way, where the mass of iHOF doping was varied. Specifically, 15.0 mg and 22.5 mg iHOF were doped into 20 wt% Nafion (1.5 g) solutions of **5.0%-iHOF-12/Nafion**, and **7.5%-iHOF-12/Nafion** composite membranes were obtained. When the doping amount of iHOF is further increased, the mechanical properties of the composite membrane decrease.

Stability experiments. The crystals of **iHOF-12** was soaked in water for 24 hours, after the water-treated, the solids were filtered out and dried at room temperature for PXRD measurements. Their chemical stability was tested as follows: the crystal of samples was dispersed in HCl or NaOH aqueous solutions with different pH values for one month (pH = 1−12), respectively. After that, the solids were filtered out and dried at room temperature for PXRD to determine their stability. We also performed a PXRD test on the crystal to determine the stability after the electrochemical impedance test.

Thermostability experiments: Thermogravimetric analysis (TGA) measurements were performed on a TGA-55 instrument from room temperature to 800 ºC at a heating rate of 10 ºC/min under N_2 atmosphere.

Proton conductivity. The electrochemical impedance test of the crystal samples was determined by sandwiching the pellets of iHOFs between two copper sheets and

then by two-electrode AC impedance spectroscopy using an electrochemical workstation (CHI 660E) in the frequency range from 1 Hz to 0.1 MHz with an alternating voltage of 5 mV. The samples were pressed into a circular cylinder with a diameter of about 7 mm on a tableting machine for 5 min under 10 MPa pressure. Their thicknesses and diameter were determined by a Vernier caliper. The temperature and relative humidity conditions are in the range of 30−100 ºC at 68% RH to 98% RH and the humidity are controlled using high and low temperature and humidity test chamber (BPHS-060A). The proton conductivity of crystal samples was obtained from the following equation: $\sigma = L/RS$, where σ is the value of proton conductivity ($S \cdot cm^{-1}$), L is the thickness (cm) of the pellet, R is the value of electrochemical impedance and S is the flat surface area (cm^2) calculated by the diameter of the circular cylinder.

The membrane samples are measured by placing them in a 2 × 2 conductivity measurement cell (shown below), their length, width and thickness are determined by vernier calipers. The proton conductivity of the membrane sample is obtained by the following equation：$\sigma = a / (R \times b \times d)$ where σ is the proton conductivity of the sample (S/cm); a is the distance between the two electrodes (cm); R is the measured impedance of the sample (Ω), b is the effective length of the membrane in the perpendicular direction to the electrodes (cm); and d is the thickness of the sample (cm).

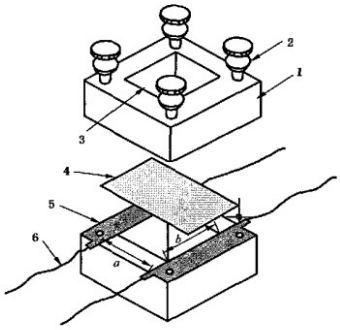

1. Polysulfone insulation frame;
2. Screw;
3. Balance the open area;
4. Membrane sample;
5. Gold plated sheet;
6. Copper wire;

For the Nyquist plots of the samples, we used an equivalent circuit (shown below) to fit the data in the Z-view software.

Activation energy (E_a) values were calculated from the Arrhenius equation: $T\sigma = \sigma_0 \exp(-E_a/kT)$, where σ_0 is the pre-exponential factor, T is temperature, k is Boltzmann constant.

Instrumentation. Powder X-ray diffraction (PXRD) measurements were carried out in Bruker D8 Advance with a Cu X-ray source over a range of 2θ = 5.0-50.0º. TGA measurements were performed on a TGA-55 instrument from room temperature to 800 ºC at a heating rate of 10 ºC/min under an air atmosphere. Scanning electron microscope tests were performed on a SU8100. The mechanical properties of the membrane are tested on CMT4202 for the tensile tester. Fourier-transform infrared (FTIR) spectra were obtained on a Bruker VECTOR-22 FTIR spectrometer in the 4000~400 cm^{-1} region with KBr pellets. Water vapor adsorption tests were performed on Bel Max instruments.

Water uptake and Swelling ratio. Water uptake and swelling ratio tests were measured to investigate the dimensional stability and hydrophilic ability of the membrane. The weights ($W_{dry,}$ g) and area (A_{dry}, cm^2) were pre-measured before testing. The area was measured by the length of the composite membrane. For the water uptake

measurements, the membranes were dried in a vacuum oven at 100 °C for 6 hours and weighed. The composite membrane was cut into pieces (1 × 1 cm^2) and then immersed into deionized water for 24 hours at room temperature. After that, the weights (W_{wet}, g) and areas (A_{wet}, cm^2) of the membrane were calculated immediately after wiping off the moisture on the surface. The water uptake and swelling rates were calculated using the following equations:

$$\text{Water uptake} = [(W_{wet} - W_{dry})/W_{dry}] \times 100\%$$

$$\text{Swelling ratio} = [(A_{wet} - A_{dry})/A_{dry}] \times 100\%$$

Ion exchange capacity. Take a sample with a mass of not less than 0.5 g, cut it into pieces, place it in a 0.1 MPa, 80 ℃ vacuum drying oven for 8 hours, take it out of the vacuum drying oven and quickly weigh its weight W, put the sample in a sealed, stir in a reagent bottle filled with saturated sodium chloride solution for 24 hours, titrate it with 0.01 mol/L sodium hydroxide solution until it is neutral, and record the volume V of sodium hydroxide solution consumed.

$$\text{IEC} = (V_{NaOH} \times C_{NaOH})/W_{Dry}$$

where C_{NaOH} ($mol \cdot L^{-1}$) is the molar concentration of the NaOH solution; V_{NaOH} (L) is the consumed volume of the NaOH solution during the titration process; and W_{Dry} (g) is the weight of the dry samples.

Methanol permeability measurement Methanol permeability of membranes was measured using liquid permeation equipment in two rooms. The membrane was cut into a round piece and sandwiched between two rooms which contained 8 M aqueous methanol solution and deionized water, respectively (shown in the figure below). The

two rooms were continuously stirred during the test. The concentration of methanol in the deionized water was periodically determined by gas chromatography (GC). Methanol permeability was calculated using the following equation:

$$C_B(t) = APC_A(t\text{-}t_0)/V_B L$$

Where A (cm^2), L (cm) and V_B (cm^3) are the diffusion area, the thickness of the membrane and the volume of permeated reservoirs, respectively. C_A and C_B ($mol \cdot L^{-1}$) are the methanol concentration in donor and receptor reservoirs, respectively. P ($cm^2 \cdot s^{-1}$) and $t\text{-}t_0$ are the methanol permeability and the time of methanol penetration, respectively.

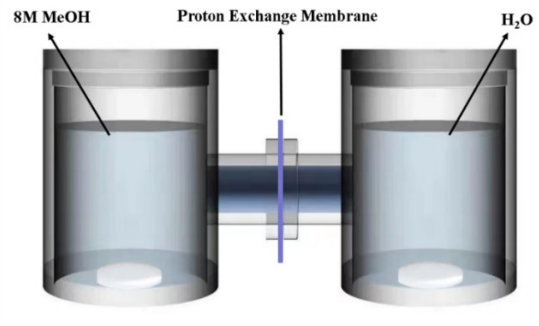

SEM and mechanical properties: Scanning electron microscope tests were performed on an SU8100. The mechanical properties of the membrane are tested on CMT4202 for tensile tester.

DMFC Performance Testing. The cell performance of the membrane was investigated using a fuel cell workstation. The membrane electrode assembly (MEA) was constructed by directly coating the catalyst slurry on the membrane to prepare the catalytic layer, which was then combined with a gas diffusion layer (GDL). The catalyst slurry is made by fully and evenly mixing platinum carbon catalyst (Johnmn Matthey, 60%), 5% Nafion solution and isopropyl alcohol. The prepared catalyst slurry was

coated on the upper and lower surfaces of the membrane, and then the membrane was bonded to the GDL layer (Toray TGP-H-060, 20 wt% PTFE) coated with conductive adhesive to obtain the MEA.

The test conditions were as follows: the effective area of the membrane was 6 cm^2, the anode side was fed with methanol aqueous solution at a concentration of 2 M and a flow rate of 4 $mL \cdot min^{-1}$, the cathode side was fed with 100% humidified atmospheric air at a flow rate of 1.2 $L \cdot min^{-1}$, and the test temperature was 80 °C. The catalyst on the anode side was a mixed Pt/Ru catalyst and on the cathode side was a mixed Pt/C catalyst.

Section S2. Single crystal X-ray diffraction analyses

Single-crystal X-ray diffraction data for compounds **iHOF-12** was collected on a Bruker SMART APEX CCD diffractometer[3] equipped with a graphite-monochromated Mo-Kα radiation (λ = 0.71073 Å) using the ω-scan technique. Data reduction was performed using SAINT and corrected for Lorentz and polarization effects. Adsorption corrections were applied using the SADABS routine.[4] All the structures were solved with direct methods (*SHELXS*)[5] and refined by full-matrix least-squares on F^2 using *OLEX2*,[6] which utilizes the *SHELXL*-2015 module.[7] All non-hydrogen atoms were refined anisotropically. Displacement parameter restraints were used in modeling the ligands. Hydrogen atoms were placed geometrically on their riding atom where possible. The contents of the solvent region are not represented in the unit cell contents in the crystal data. Crystal data containing space group, lattice parameters, and other relevant information for the title complex are summarized in Table S1. More details on the crystallographic data are given in the X-ray crystallographic files in CIF format. Full details of the structure determinations have been deposited with Cambridge Crystallographic Data Center under reference number CCDC 2233365 for **iHOF-12**, and is available free of charge from CCDC.

Table S1. Crystal structure data and refinement details of **iHOF-12**.

Compound	iHOF-12
Empirical formula	$C_{45}H_{44}N_8O_{14}S_4$
Formula weight	1049.12
Temperature / K	143.0
Wavelength / Å	0.71073
Crystal system	tetragonal
Space group	*I*-4
a/Å	24.9659(16)
b/Å	24.9659(16)
c/Å	7.1345(7)
α/°	90.00
β/°	90.00
γ/°	90.00
Volume/Å^3	4446.9(6)
Z	4
Density (calculated) / g·cm^{-3}	1.567
Absorption coefficient / mm^{-1}	0.295
F(000)	2184.0
Reflections collected	19880
Independent reflections	3923 (R_{int} = 0.0751, R_{sigma} = 0.0551)
Data/restraints/parameters	3923/19/352
Goodness-of-fit on F^2	1.068
$^aR_1$, $^bwR_2$ [$I > 2\sigma(I)$]	0.0476/0.1128
$^aR_1$, $^bwR_2$ (all data)	0.0577/0.1183
Largest diff. peak and hole/ e.Å^{-3}	0.42/-0.29
CCDC number	2233365

$^aR_1 = \sum||F_o| - |F_c||/\sum|F_o|$. $^bwR_2 = \{\sum[w(F_o^2 - F_c^2)^2]/\sum[w(F_o^2)^2]\}^{1/2}$

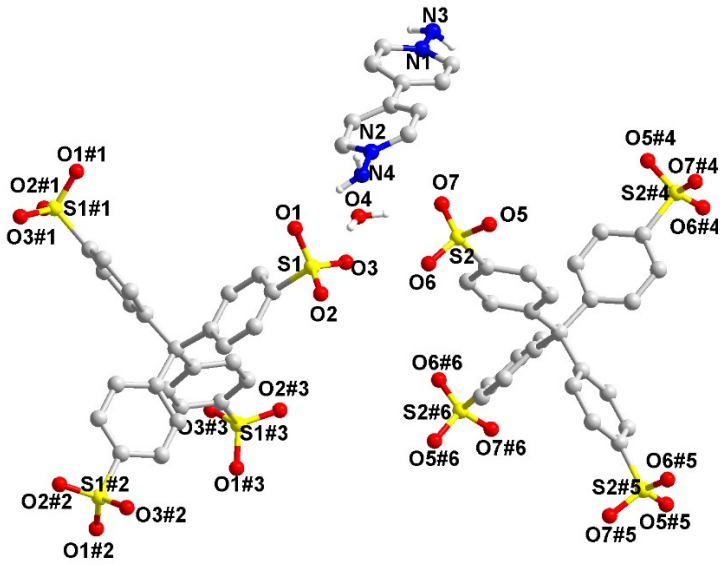

Figure S1. The asymmetric unit of **iHOF-12**. Symmetry codes: #1: –*x*, 1 − *y*, *z*; #2: 1/2 – *y*, 1/2 + *x*, 5/2 – *z*; #3: –1/2 + *y*, 1/2 – *x*, 5/2 – *z*; #4: 1 – *x*, 1 – *y*, *z*; #5: *y*, 1– *x*, 2 – *z*; #6: 1 – *y*, *x*, 2 – *z*.

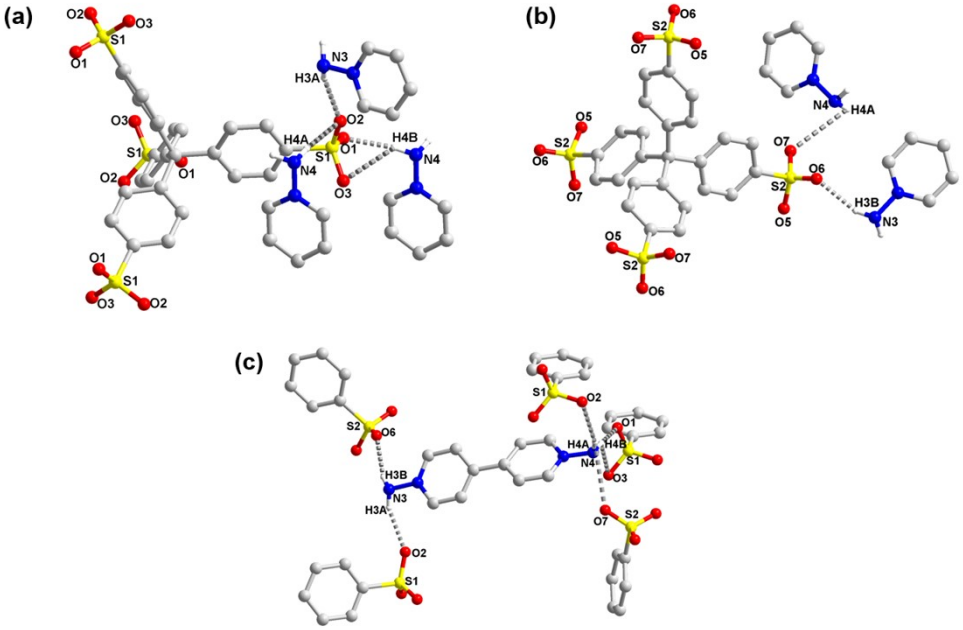

Figure S2. The hydrogen bond interactions between TSM^{4-} and $DBpy^{2+}$. (a) the type I of TSM^{4-}; (b) the type II of TSM^{4-}; (c) $DBpy^{2+}$ moieties.

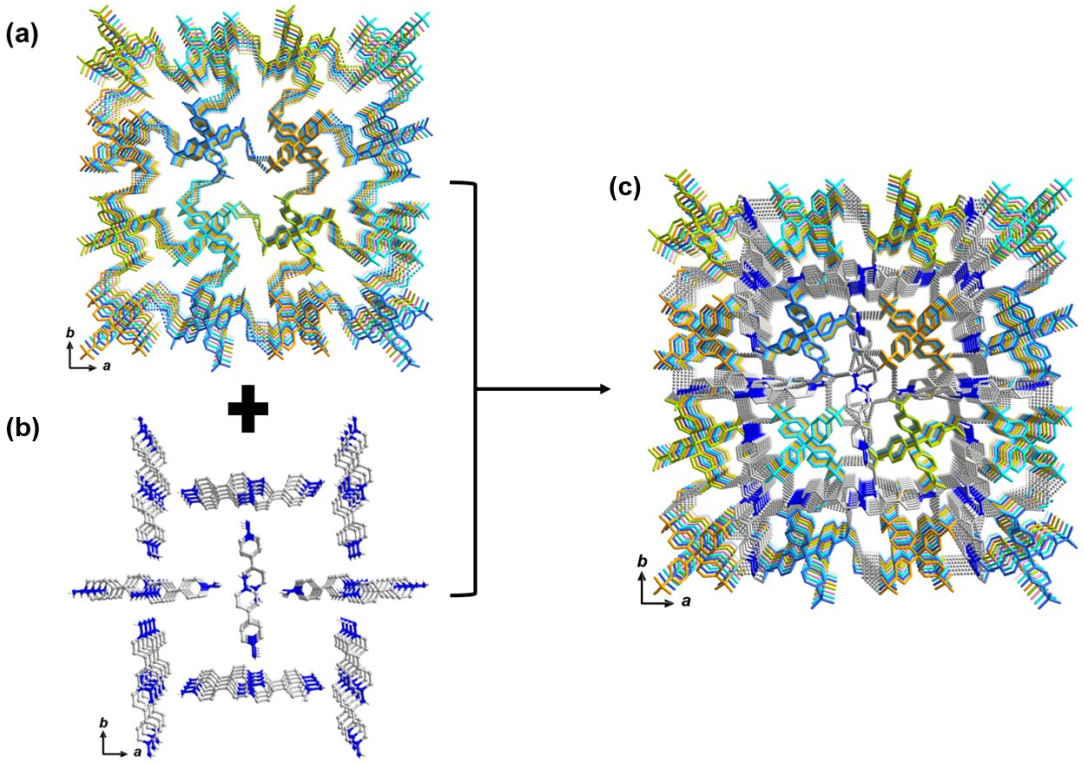

Figure S3. (a) View along the *c*-axis showing the 5-fold interpenetrated structure of TSM^{4-} and water molecules. (b) The distribution of $DBpy^{2+}$ moieties in the structure. (c) The integral 3D packing supramolecular structure.

Section S3. TGA patterns

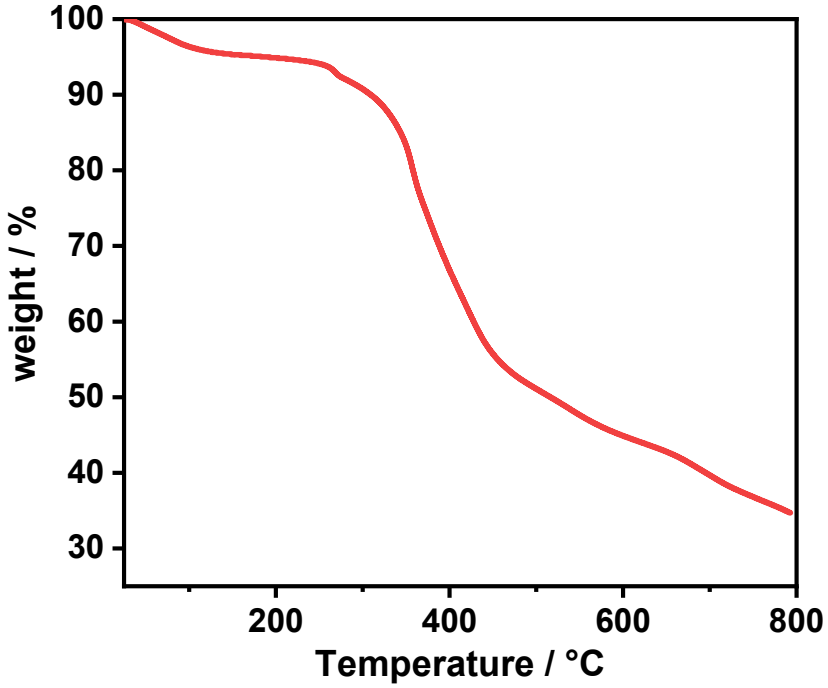

Figure S4. TGA plots of **iHOF-12.**

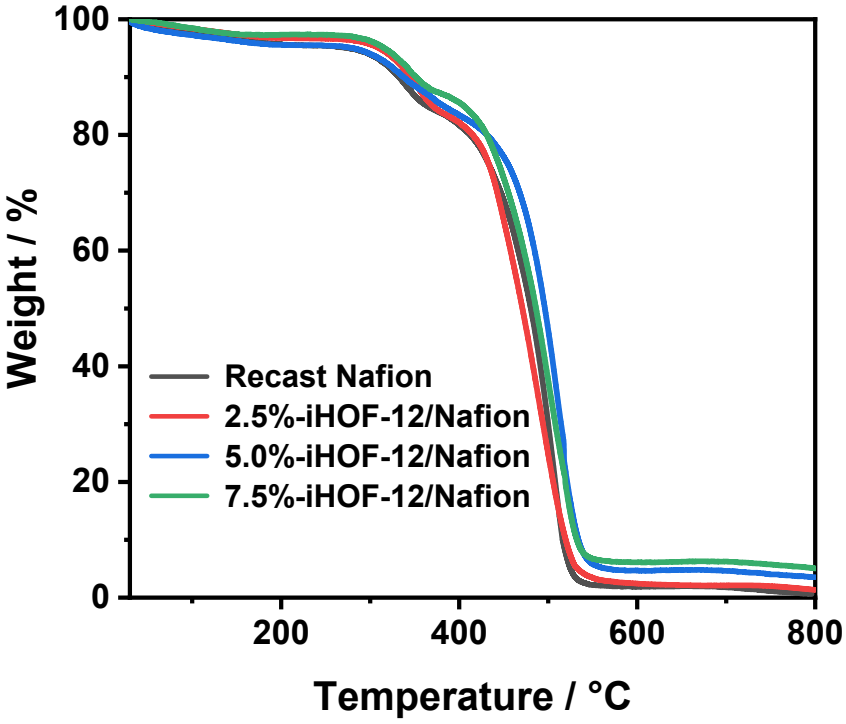

Figure S5. TGA plots of recast Nafion, **2.5%-iHOF-12/Nafion**, **5.0%-iHOF-12/Nafion**, **7.5%-iHOF-12/Nafion** membranes.

Section S4. FTIR patterns

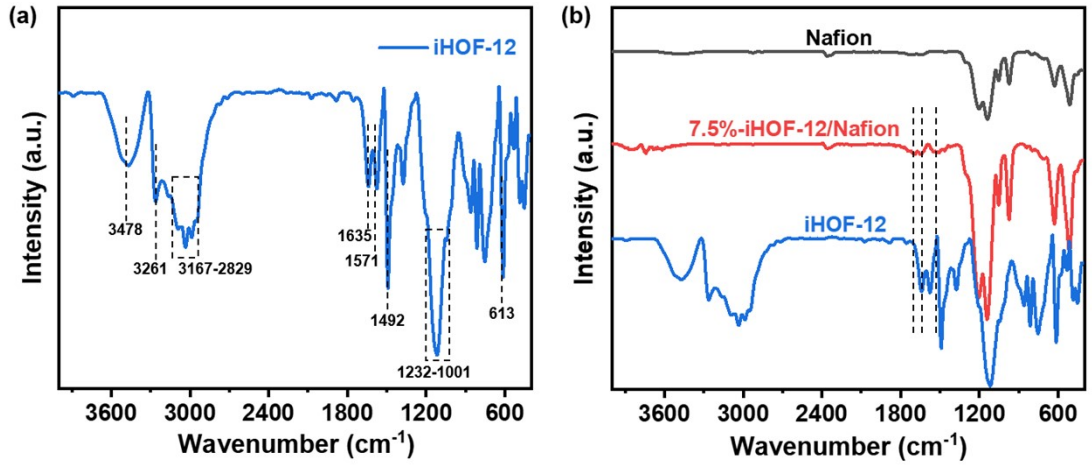

Figure S6. FTIR spectra of the (a) **iHOF-12**; (b) **iHOF-12**, Nafion, and **7.5%-iHOF-12/Nafion** from 4000 to 400 cm^{-1}.

Section S5. Scanning Electron Microscope

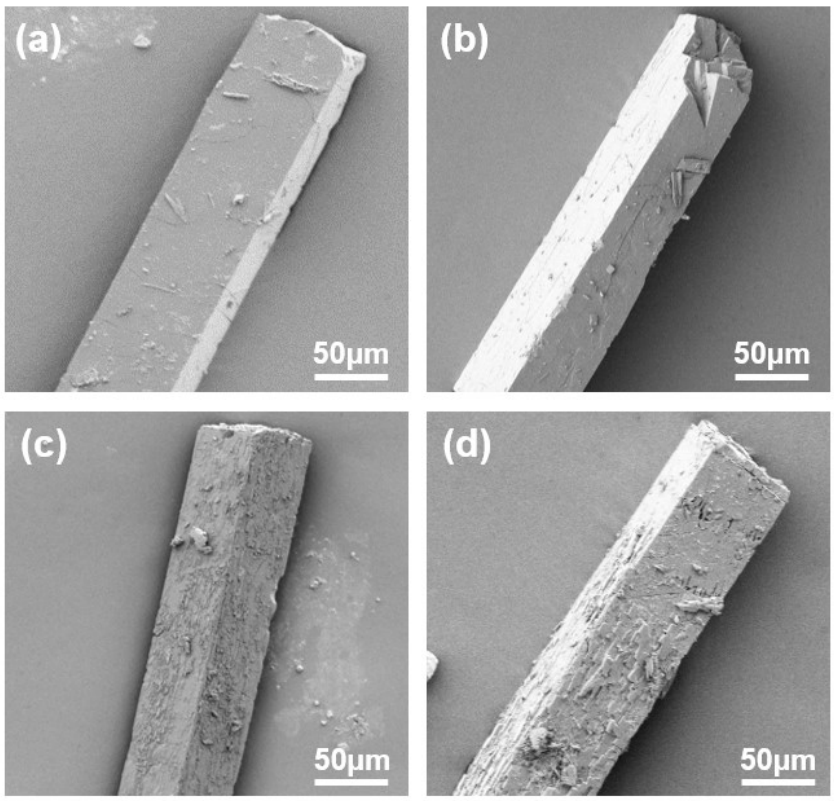

Figure S7. (a) Morphology of SEM images of (a) synthesized **iHOF-12**; (b) **iHOF-12** after one month in water; (c) **iHOF-12** after one month immersion in pH=1 solution; (d) **iHOF-12** after one month immersion in pH=12 solution.

Section S6. Proton conductivity

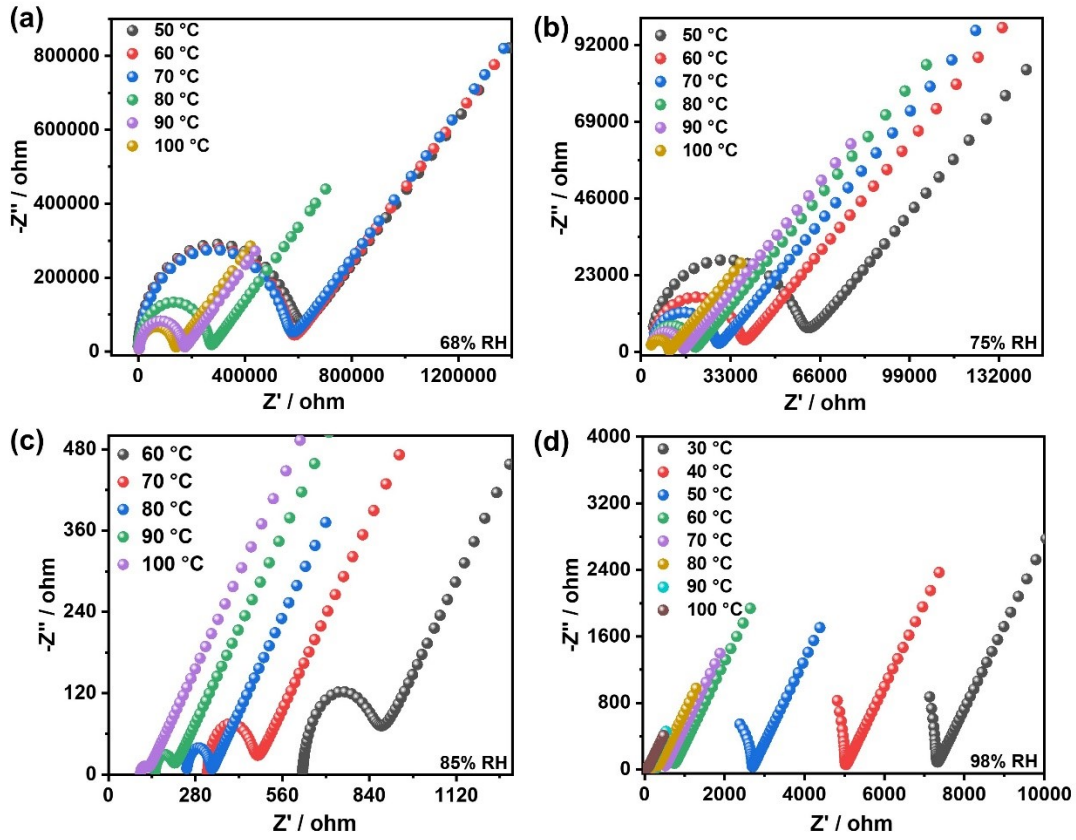

Figure S8. (a) The Nyquist plot of **iHOF-12** at 68% RH. (b) The Nyquist plot of **iHOF-12** at 75% RH. (c) The Nyquist plot of **iHOF-12** at 85% RH. (d) The Nyquist plot of **iHOF-12** at 98% RH.

Table S2. Proton conductivities ($S \cdot cm^{-1}$) for **iHOF-12** at 60−100 ºC and different RH.

	60 °C	70°C	80°C	90°C	100°C
68%RH	1.13×10^{-5}	3.65×10^{-4}	6.48×10^{-4}	7.36×10^{-4}	3.38×10^{-3}
75%RH	1.21×10^{-5}	1.89×10^{-3}	2.18×10^{-3}	2.45×10^{-3}	3.49×10^{-3}
85%RH	1.17×10^{-4}	1.98×10^{-3}	2.31×10^{-3}	2.97×10^{-3}	6.18×10^{-3}
93%RH	1.32×10^{-3}	2.01×10^{-3}	2.98×10^{-3}	5.23×10^{-3}	7.22×10^{-3}
98%RH	1.72×10^{-3}	2.41×10^{-3}	3.55×10^{-3}	8.87×10^{-3}	1.23×10^{-2}

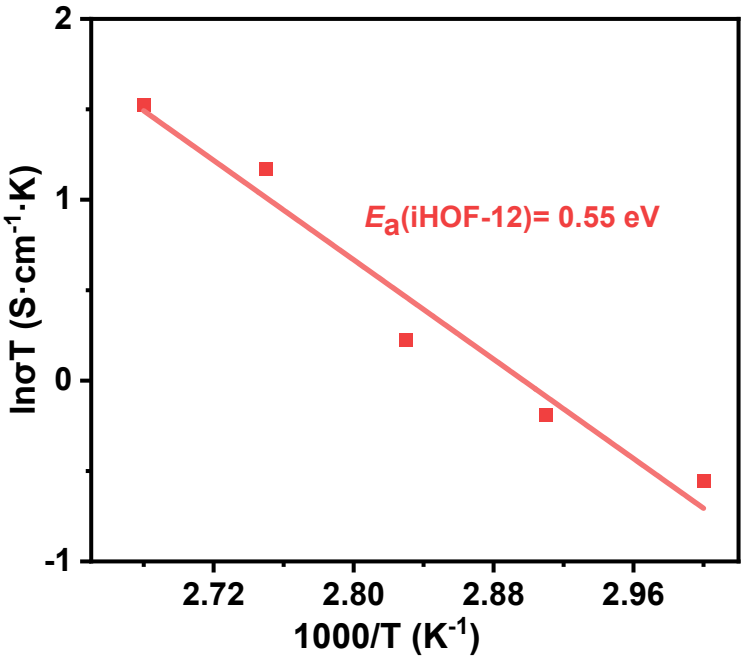

Figure S9. Arrhenius diagrams of **iHOF-12** at 98% RH.

Section S7. Digital Imaging

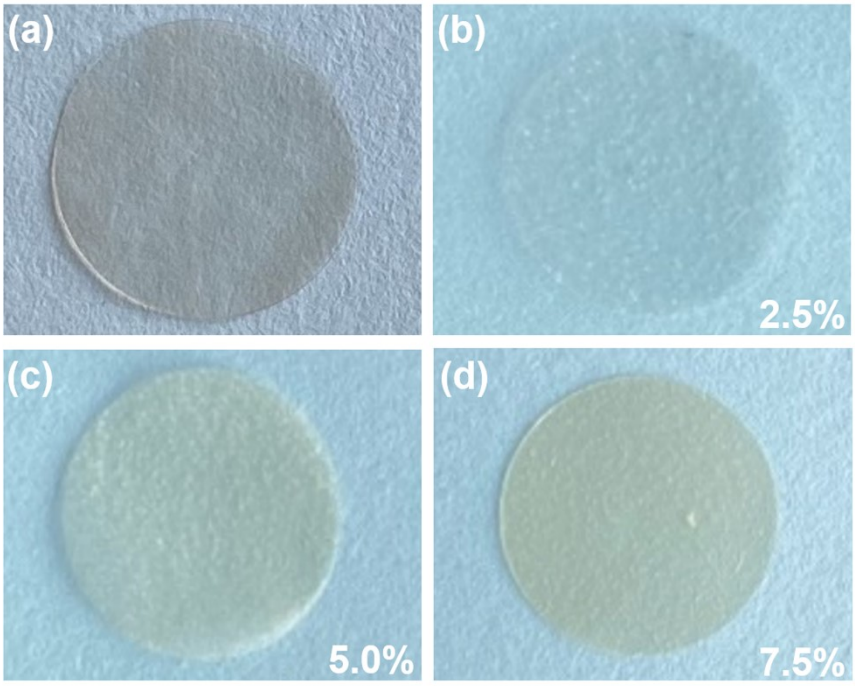

Figure S10. (a) The digital images of the recast Nafion membrane. The digital images of **iHOF-12/Nafion** composited membranes: (b) **2.5%-iHOF-12/Nafion**; (c) **5.0%-iHOF-12/Nafion**; (d) **7.5%-iHOF-12/Nafion**.

Section S8. Scanning Electron Microscope and AFM

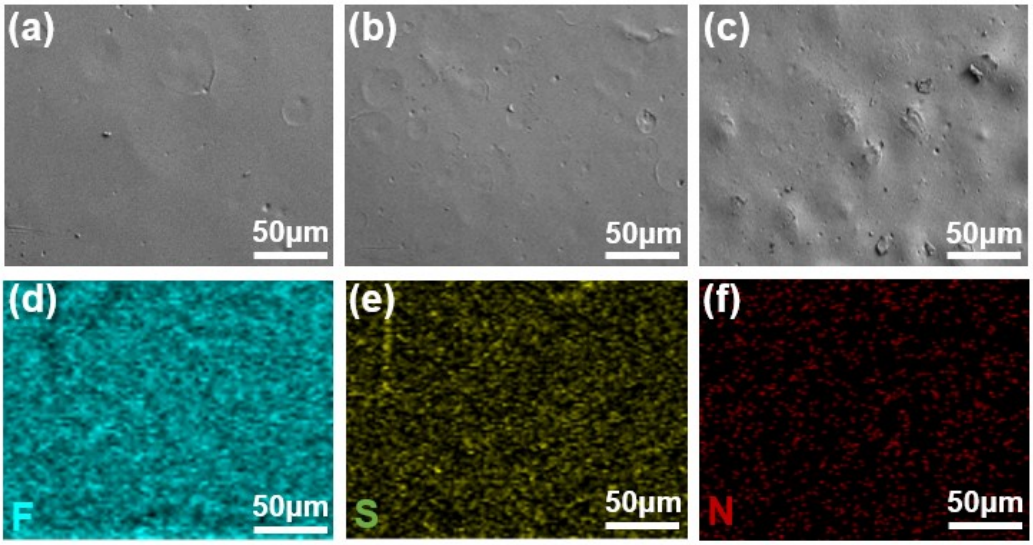

Figure S11. (a−c) The SEM images of **2.5%-iHOF-12/Nafion**, **5.0%-iHOF-12/Nafion,** and **7.5%-iHOF-12/Nafion**, respectively. (d−f) Image mapping of elements corresponding to F, S, and N in the **7.5%-iHOF-12/Nafion** membrane.

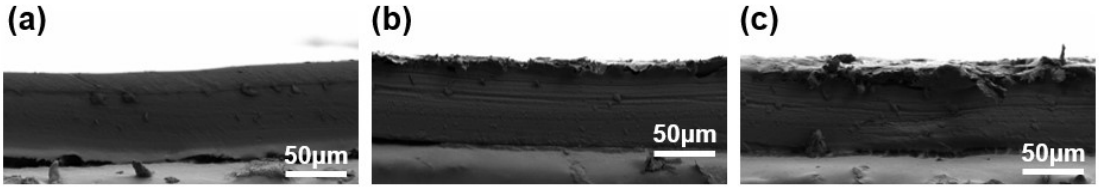

Figure S12. SEM image of the cross-section of (a) **2.5%-iHOF-12/Nafion** composite membrane. (b) **5.0%-iHOF-12/Nafion** composite membrane. (c) **7.5%-iHOF-12/Nafion** composite membrane.

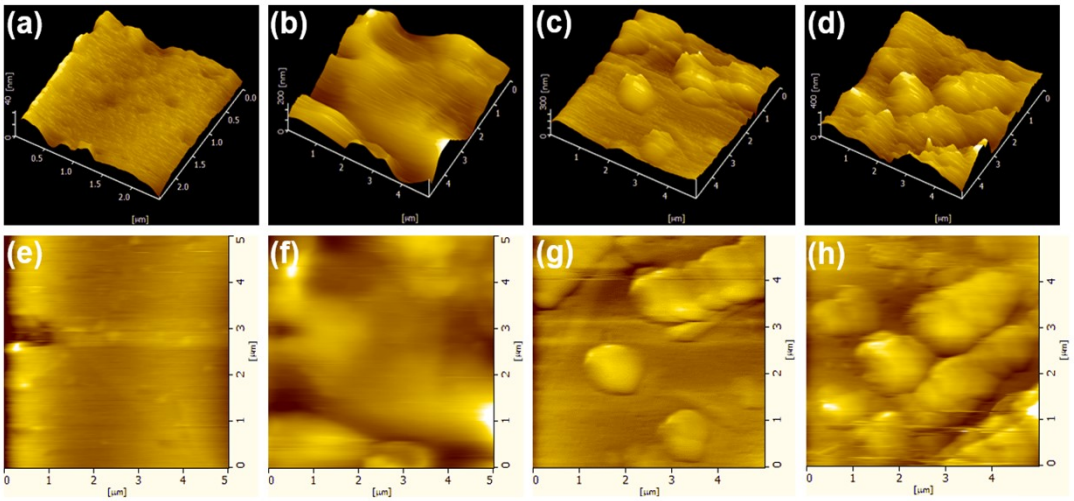

Figure S13. AFM topography images of (a) recast Nafion membrane; (b) **2.5%-iHOF-12/Nafion** membrane; (c) **5.0%-iHOF-12/Nafion** membrane; (d) **7.5%-iHOF-12/Nafion** membrane. The AFM phase images of (e) recast Nafion membrane; (f) **2.5%-iHOF-12/Nafion** membrane; (g) **5.0%-iHOF-12/Nafion** membrane; (h) **7.5%-iHOF-12/Nafion** membrane.

Section S9. Mechanical stability

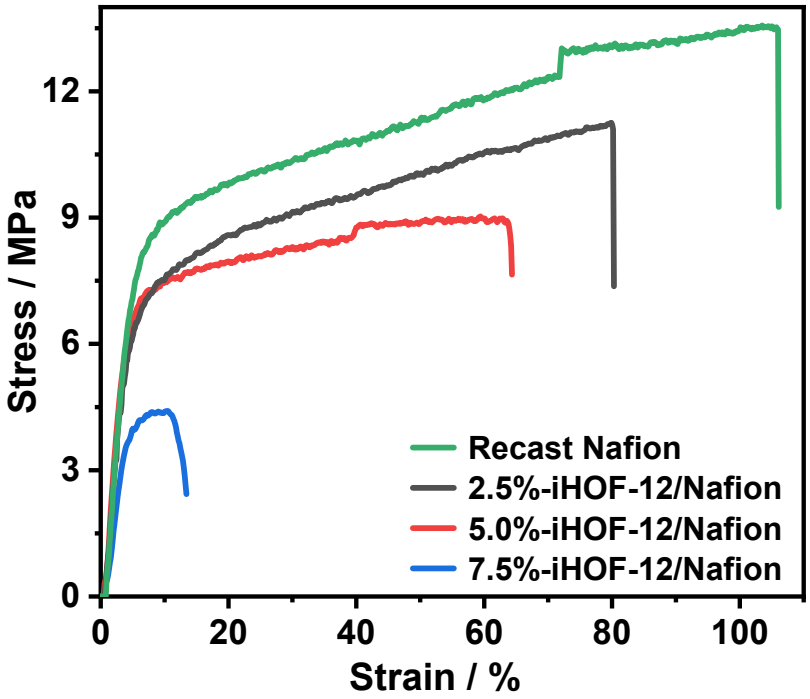

Figure S14. Tensile plots of recast Nafion membrane and composite membranes.

Section S10. Water Uptake, Swelling Ratio and IEC of Hybrid Membranes

Table S3. Water uptake, Swelling ratio, IEC of different membranes at 25 °C.

Membranes	Water uptake/ (%)	Area Swelling / (%)	IEC /mmol·g^{-1}
Recast Nafion	38.25	21.80	0.86
2.5%-iHOF-12/Nafion	31.23	17.85	0.93
5.0%-iHOF-12/Nafion	27.10	14.56	1.02
7.5%-iHOF-12/Nafion	22.25	10.25	1.15

Section S11. Proton conductivity of membrane and battery performance

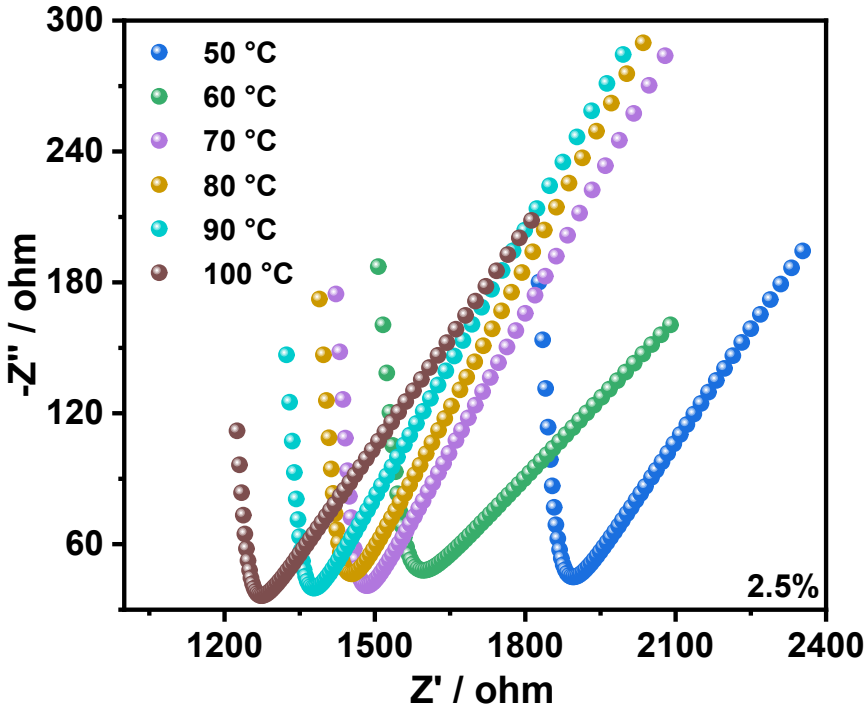

Figure S15. The Nyquist plot of **2.5%-iHOF-12/Nafion** membrane at 98% RH and 100 °C.

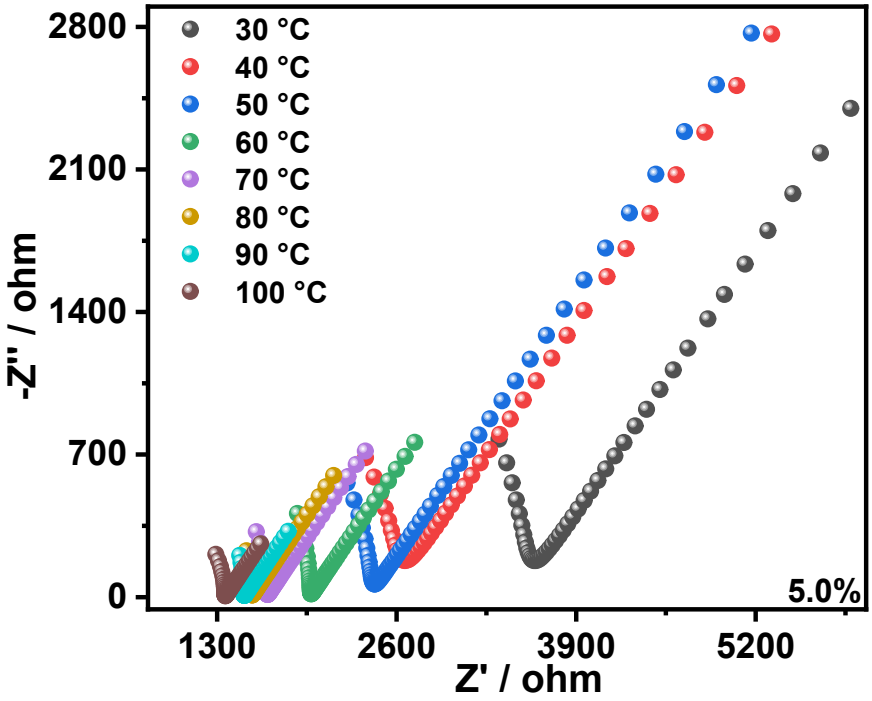

Figure S16. The Nyquist plot of **5.0%-iHOF-12/Nafion** membrane at 98% RH and 100 °C.

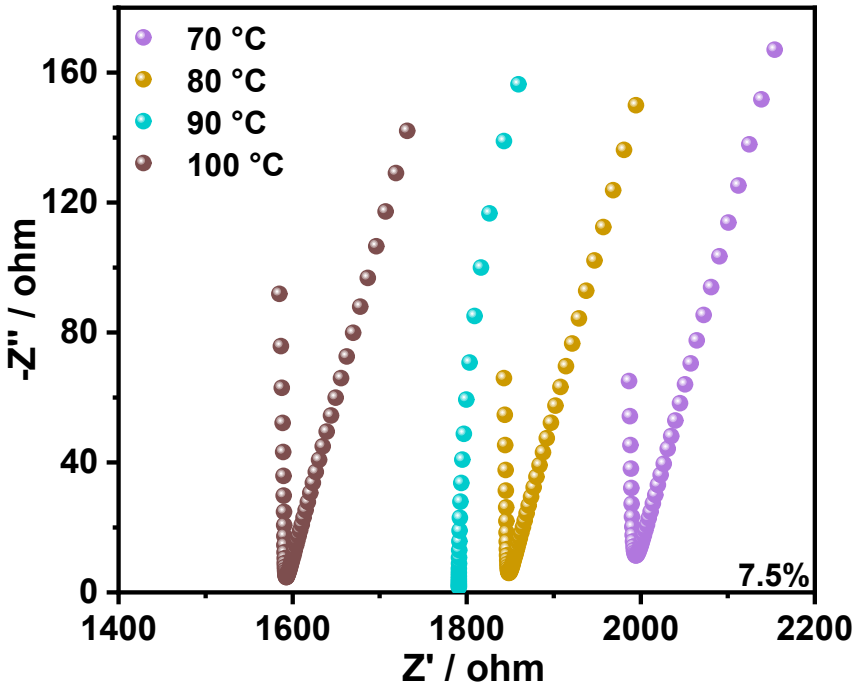

Figure S17. The Nyquist plot of **7.5%-iHOF-12/Nafion** membrane at 98% RH and 100 °C.

Table S4. Proton conductivity of composite membranes with different doping ratios at different temperatures.

Membranes	70 °C	80 °C	90 °C	100 °C
2.5%-iHOF-12/Nafion	4.2×10^{-2}	6.3×10^{-2}	7.5×10^{-2}	9.0×10^{-2}
5.0%-iHOF-12/Nafion	5.3×10^{-2}	7.6×10^{-2}	8.5×10^{-2}	9.3×10^{-2}
7.5%-iHOF-12/Nafion	8.5×10^{-2}	9.0×10^{-2}	9.8×10^{-2}	1.2×10^{-1}

Section S12. DMFC Performance

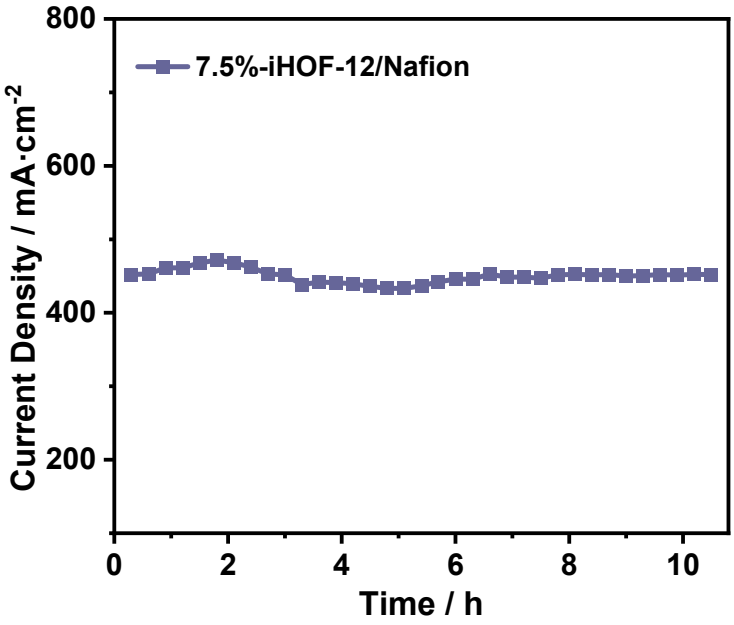

Figure S18. Performance stability of **7.5%-Ihof-12/Nafion** composite membranes at 80°C and 100% RH for 10 hours.

Table S5. The maximum power density and proton conductivity of modified Nafion membrane for DMFCs from this study compared to other works.

Membranes	σ (S·cm^{-1})	Power density (mW·cm^{-2})	*ref*
p-BPAF@ Nafion-7.5	0.256	111.53 (80 ºC)	8
Nafion-Bi_{12}-3%	0.386	110.2 (80 ºC)	9
7.5%-iHOF-12/Nafion	0.12	72.2 (80 ºC)	This work
CBA/Nafion-PVA	0.110	68.7 (80 ºC)	10
GO nanosheet /Nafion	0.06	64.38 (80 ºC)	11
X-Nafion@POSS-12	0.121	34.93 (80 ºC)	12
NF/S-GO-MOR 0.05	0.0865	29.55 (70 ºC)	13
Nafion-PDDA-GO	0.023	28 (25 ºC)	14
Nafion 117	0.108	12.05 (80 ºC)	8
Nafion/Pani-2	0.0325	8.75 (20 ºC)	15
N/Pd-SiO_2-3	0.024	8.30 (75 ºC)	8
MOR/NF	0.0494	6.00 (75 ºC)	16
ANA/NF	0.0501	4.0 (75 ºC)	17

Section S13. References

[1] S. Zhang, J. Fu, S. Das, K. Ye, W. Zhu, T. Ben, *Angew. Chem. Int. Ed*. **2022**, *61*, e202208660.

[2] J. Downes, *J. Chem. Soc. C*. **1967**, 2192-2193.

[3] S. SMART, *Bruker Analytical X-Ray. Madison*. **1997**.

[4] G. M. Sheldrick, *Germany*. **1996**.

[5] G. M. Sheldrick, *Acta Cryst. A*. **2008**, *64*, 112-122.

[6] O. V. Dolomanov, L. J. Bourhis, R. J. Gildea, J. A. Howard, H. Puschmann, *J. Appl. Cryst.* **2009**, *42*, 339-341.

[7] G. M. Sheldrick, *Acta Cryst*. C. **2015**, *71*, 3-8.

[8] C. Ru, Y. Gu, Y. Duan, C. Zhao, H. Na, *J. Membr. Sci*. **2019**, *573*, 439-447.

[9] B. Liu, B. Hu, J. Du, D. Cheng, H. Y. Zang, X. Ge, Z. Su, *Angew. Chem. Int. Ed.* **2021**, *60*, 6076-6085.

[10] Y. Li, L. Liang, C. Liu, Y. Li, W. Xing, J. Sun, *Adv.Mater.* **2018**, *30*, 1707146.

[11] L. S. Wang, A. N. Lai, C. X. Lin, Q. G. Zhang, A. M. Zhu, Q. L. Liu, *J. Membrane. Sci.* **2015**, *492*, 58-66.

[12] Z. Li, X. Hao, G. Cheng, S. Huang, D. Han, M. Xiao, Y. Meng, *J. Membr. Sci*. **2021**. *640*, 119798.

[13] P. Prapainainar, N. Pattanapisutkun, C. Prapainainar, P. Kongkachuichay, *Int. J. Hydrogen. Energ*. **2019**, *44*, 362-378.

[14] T. Yuan, L. Pu, Q. Huang, H. Zhang, X. Li, H. Yang, *Electrochim Acta.* **2014**, *117*, 393-397.

[15] H. S. Thiam, W. R. W. Daud, S. K. Kamarudin, A. B. Mohamad, A. A. H. Kadhum, K. S. Loh, E. H. Majlan, I*nt. J. Hydrogen Energy*. **2013**, *38*, 9474-9483.

[16] C. Y. Chen, J. I. Garnica-Rodriguez, M. C. Duke, R. F. Dalla Costa, A. L. Dicks, J. C. D. Costa, *J. Power Sources*. **2007**, *166*, 324-330.

[17] P. Prapainainar, Z. Du, P. Kongkachuichay, S. M. Holmes, C. Prapainainar, *Appl. Surf. Sci*. **2017**, *421*, 24-41.